

Koopmans-compliant functionals and potentials and their application to the GW100 test-set

Nicola Colonna,^{*,†} Ngoc Linh Nguyen,^{†,‡} Andrea Ferretti,[¶] and Nicola Marzari[†]

[†]*Theory and Simulation of Materials (THEOS)*

and National Centre for Computational Design and Discovery of Novel Materials (MARVEL), École Polytechnique Fédérale de Lausanne, 1015 Lausanne, Switzerland

[‡]*Institute for Molecular Engineering, University of Chicago, 5640 South Ellis Avenue, Chicago, Illinois 60637, USA*

[¶]*Centro S3, CNR-Istituto Nanoscienze, 41125 Modena, Italy*

E-mail: nicola.colonna@epfl.ch

Abstract

Koopmans-compliant (KC) functionals have been shown to provide accurate spectral properties through a generalized condition of piece-wise linearity of the total energy as a function of the fractional addition/removal of an electron to/from any orbital. We analyze the performance of different KC functionals on the GW100 test-set, comparing the ionization potentials (as opposite of the energy of the highest occupied orbital) of these 100 molecules to those obtained from CCSD(T) total energy differences, and experimental results, finding excellent agreement with a mean absolute error of 0.20 eV for the KIPZ functional, that is state-of-the-art for both DFT-based calculations and many-body perturbation theory. We highlight similarities and differences between KC functionals and other electronic-structure approaches, such as dielectric-dependent hybrid functionals and G_0W_0 , both from a theoretical and from a practical point of

view, arguing that Koopmans-compliant potentials can be considered as a local and orbital-dependent counterpart to the electronic GW self-energy, albeit already including approximate vertex corrections.

1 Introduction

Computational spectroscopy is a valuable tool to support and complement experiments and drive, nowadays, the discovery of novel materials for diverse applications.¹⁻⁴ Although reasonably accurate spectral properties can be obtained using quantum chemistry wave-function methods or many-body perturbation theory⁵ (MBPT), these approaches have an unfavorable scaling with the size of the system often constraining one to study only relatively small or simple systems. For this reason faster approaches based on density-functional theory (DFT), Hartree-Fock, or a mixture of the two, as in hybrid functionals, are often used. Δ self-consistent “ Δ SCF” calculations based on standard density-functional approximations (DFAs) are also quite accurate for small-size systems, but fails in the solid-state limit; single-particle energies from Hartree-Fock are protected by Koopmans’ theorem and can be interpreted as energy removals or additions, but lack relaxation effects, usually leading to an overestimation of the first ionization potential (IP), an underestimation of the electron affinity (EA) and consequently to overestimation of the fundamental gap. The exact exchange-correlation (xc) energy functional of Kohn-Sham (KS) density functional theory would provide exactly the first ionization potential of a system of interacting electrons, as the opposite of the energy of the highest occupied molecular orbital (HOMO) of the auxiliary KS system^{6,7} (in addition, of course, of providing it as a total energy difference between the neutral system with N electrons and the ionized one with $N - 1$ electrons). However (i) KS energies other than the HOMO have no obvious connection with charged excitations of the real system (see e.g. Ref. 8 for an in depth discussion about the connection between KS eigenvalues and vertical ionization potentials), and (ii) not even the first ionization potential is correctly reproduced when standard local or semi-local DFAs are used. This latter

failure can be understood in terms of the deviation from the expected piece-wise linearity (PWL) of the exact energy functional as a function of the number of particles, first discussed by Perdew-Parr-Levy-Baldur⁶ (PPLB). Diverse xc functional developments^{9–20} are indeed guided by such a fundamental condition, with the aim of correcting the spurious self-interaction error present in almost all DFAs and get accurate prediction of frontier orbital energies from single-particle energies.

In this respect, Koopmans’ compliant (KC) functionals have been introduced^{11,12,21} to purify standard density-functional approximations from self-interaction errors deriving from the lack of PWL. In this formulation, a generalized PWL condition is imposed to the total energy as a function of the fractional occupation of *any* orbital in the system, thus extending the standard PPLB linearity condition (valid only for the highest occupied state) to the entire electronic manifold. This ansatz results in a beyond-DFT orbital-density dependent functionals with enough flexibility to correctly reproduce both ground state and spectral properties. Infact, while the ground state energies are very close or identical to those of the starting functional,²¹ we argued²² that for the spectral properties the orbital-dependent KC potentials act as a quasiparticle approximation to the spectral potential,^{23–25} i.e. the local and frequency-dependent potential sufficient to correctly describe the local spectral density $\rho(\mathbf{r},\omega)$. To further support this picture we present in this work a detailed analysis of the KC orbital-dependent potentials and establish a connection with more complex electronic-structure methods, and in particular with the well-known GW approximation²⁶ in the framework of many-body perturbation theory. We provide additional evidence that, in a localized representation of the electronic manifold, the orbital-dependent KC potentials provide simplified but yet accurate approximations to the non-local and frequency-dependent self-energy. We finally analyze the performance of the KC functionals on the GW100 test set;²⁷ comparing our results against state-of-the-art GW calculations, accurate quantum chemistry methods, and experiments finding overall an excellent agreement, even more remarkable as obtained with a functional theory of the orbital densities.

2 Koopmans-compliant functionals

In this Section we review the basic features of KC functionals and we refer to Refs. 21, 28,29 for an extensive discussion of the approach, that is based on the three concepts of linearization, screening, and localization.

Linearization. The basic ansatz behind the KC functionals is to enforce a generalized criterion of piece-wise linearity to the total energy as a function of the fractional occupation of any orbital in the system. This is a generalization of the well-know PWL of the total energy as a function of the number of particles⁶ (or, equivalently, as a function of the fractional occupation of the highest occupied state) to the entire electronic manifold. This is achieved in two steps: starting from any non-linear density functional E^{DFT} and for each orbital $\phi_{i\sigma}$ first (i) the “bare” or “unscreened” Koopmans corrections $\{\Pi_{i\sigma}^u\}$ are applied to enforce linearity as a function of each spin-orbital occupation $f_{i\sigma}$ in a *frozen orbital picture*, i.e. assuming that all other electrons do not respond when a particle is added/removed from the system. Then (ii) relaxation effects are captured by orbital-dependent screening parameters $\{\alpha_{i\sigma}\}$ for the bare corrections, leading to the general form of the KC functionals as:

$$E^{\text{KC}} = E^{\text{DFT}} + \sum_{i\sigma} \alpha_{i\sigma} \Pi_{i\sigma}^u. \quad (1)$$

The corrections $\{\Pi_{i\sigma}^u\}$ remove, in a frozen-orbital picture and for each orbital $\phi_{i\sigma}$, the “Slater” non-linear behavior of the underlying functional as a function of the occupation $f_{i\sigma}$ of the orbital at hand, and replace it with a linear Koopmans term; that is

$$\Pi_{i\sigma}^u(f_{i\sigma}) = - \int_0^{f_{i\sigma}} \langle \phi_{i\sigma} | H^{\text{DFT}}(s) | \phi_{i\sigma} \rangle ds + f_{i\sigma} \eta_{i\sigma} \quad (2)$$

$$= - \text{Slater} + \text{Koopmans} \quad (3)$$

where $H^{\text{DFT}}(s)$ is the KS-DFT Hamiltonian calculated at a density where the orbital $\phi_{i\sigma}$ has occupation s , and $\eta_{i\sigma}$ is the slope of the linear Koopmans term. The slope $\eta_{i\sigma}$ can be chosen

either following Slater’s intuition (i.e. choosing $\eta_{i\sigma}$ as the orbital energy at occupation 1/2), or enforcing in a functional form the Δ SCF concept, i.e. choosing the slope as the total energy difference between two adjacent points at integer occupations ($f_{i\sigma} = 0$ and $f_{i\sigma} = 1$). In the latter case one obtains the KI (“I” stands for integral) correction, that reads

$$\begin{aligned} \Pi_{i\sigma}^{\text{uKI}} &= - \int_0^{f_{i\sigma}} \langle \phi_{i\sigma} | H^{\text{DFT}}(s) | \phi_{i\sigma} \rangle ds + f_{i\sigma} \int_0^1 \langle \phi_{i\sigma} | H^{\text{DFT}}(s) | \phi_{i\sigma} \rangle ds = \\ &= - \left(E_{\text{Hxc}}^{\text{DFT}}[\rho] - E_{\text{Hxc}}^{\text{DFT}}[\rho - \rho_{i\sigma}] \right) + f_{i\sigma} \left(E_{\text{Hxc}}^{\text{DFT}}[\rho - \rho_{i\sigma} + n_{i\sigma}] - E_{\text{Hxc}}^{\text{DFT}}[\rho - \rho_{i\sigma}] \right) \end{aligned} \quad (4)$$

where $E_{\text{Hxc}}^{\text{DFT}}$ is the Hartree and exchange-and-correlation energy associated to the underlying functional, $\rho_{i\sigma}(\mathbf{r}) = f_{i\sigma} |\phi_{i\sigma}(\mathbf{r})|^2 = f_{i\sigma} n_{i\sigma}(\mathbf{r})$ is the orbital density at occupation $f_{i\sigma}$, $n_{i\sigma}(\mathbf{r})$ is the orbital density at occupation 1, and $\rho(\mathbf{r}) = \sum_{i\sigma} \rho_{i\sigma}(\mathbf{r})$ is the total charge density. From the definition above it can be seen that at integer occupations the $\Pi_{i\sigma}^{\text{uKI}}$ correction vanishes and the KI functional becomes identical to its base functional, independently from the screening coefficients. The KI functional thus preserves exactly the potential energy surface of the base functional it started from; its value at fractional occupations is instead different and so are the derivatives everywhere, including at integer occupations, and therefore the spectral properties. If instead of the DFT energy difference we choose the Perdew-Zunger (PZ) self-interaction corrected³⁰ (SIC) one, i.e. $\eta_{i\sigma} = \int_0^1 \langle \phi_{i\sigma} | H_{i\sigma}^{\text{PZ}}(s) | \phi_{i\sigma} \rangle ds$, we obtain the KIPZ correction:

$$\begin{aligned} \Pi_{i\sigma}^{\text{uKIPZ}} &= - \int_0^{f_{i\sigma}} \langle \phi_{i\sigma} | H^{\text{DFT}}(s) | \phi_{i\sigma} \rangle ds + f_{i\sigma} \int_0^1 \langle \phi_{i\sigma} | H_{i\sigma}^{\text{PZ}}(s) | \phi_{i\sigma} \rangle ds \\ &= \Pi_{i\sigma}^{\text{KI}} - f_{i\sigma} E_{\text{Hxc}}[n_{i\sigma}] \end{aligned} \quad (5)$$

where $H_{i\sigma}^{\text{PZ}}(s) = H^{\text{DFT}}(s) - v_{\sigma, \text{Hxc}}^{\text{DFT}}[s |\phi_{i\sigma}(\mathbf{r})|^2]$ is the PZ-SIC Hamiltonian, with $-v_{\sigma, \text{Hxc}}^{\text{DFT}}$ the PZ-SIC correction for the orbital $\phi_{i\sigma}$ occupied by s electrons. The KIPZ functional inherits from the PZ-SIC functional the important property of being one-electron self-interaction free (at least in its unscreened form, that is the exact one for one-electron systems), while at the

same time it preserves the linear behavior of the energy also in many-particle systems and thus is also (approximately) free from the many-body self-interaction error.³¹

Screening. If all $\alpha_{i\sigma} = 1$ the energy functional in Eq. (1) is by construction linear in each orbital occupation $f_{i\sigma}$ if one neglects orbitals relaxation. This is analogous to realizing a DFT equivalent of the “restricted” Koopmans theorem in Hartree-Fock theory, and it is not enough to guarantee the linearity of the functional in the general case. To include the response of the system to the ionization process (change in the occupation) embodied in the $\Pi_{i\sigma}^{\text{KC}}$ term, *screening parameters* $\{\alpha_{i\sigma}\}$ are introduced for each orbital. By definition the screening parameters transform the unrelaxed Koopmans’ correction $\Pi_{i\sigma}^{\text{u}}$ into the fully relaxed one $\Pi_{i\sigma}^{\text{r}}$. The latter can be calculated by self-consistent finite differences,²⁸ or by linear response²⁹ as if a tiny fraction of an electron were removed/added from/to a given orbital. In this case a second-order Taylor expansion in the orbital occupations $f_{i\sigma}$ can be used to approximate the relaxed and unrelaxed KC corrections, and the screening coefficient $\alpha_{i\sigma}$ associated to each orbital $\phi_{i\sigma}$ can be calculated as²⁹

$$\alpha_{i\sigma} = \frac{\Pi_{i\sigma}^{\text{r}}}{\Pi_{i\sigma}^{\text{u}}} \xrightarrow{2^{\circ} \text{ order}} \frac{[d^2 E^{\text{app}}/df_{i\sigma}^2]_{\text{relax}}}{[d^2 E^{\text{app}}/df_{i\sigma}^2]_{\text{unrelax}}} = \frac{\langle n_{i\sigma} | [\tilde{\varepsilon}^{-1} f_{\text{Hxc}}]^{\sigma\sigma} | n_{i\sigma} \rangle}{\langle n_{i\sigma} | f_{\text{Hxc}}^{\sigma\sigma} | n_{i\sigma} \rangle} \quad (6)$$

where

$$\Pi_{i\sigma}^{\text{u}} = \frac{1}{2} f_{i\sigma} (1 - f_{i\sigma}) \left. \frac{d^2 E^{\text{app}}}{df_{i\sigma}^2} \right|_{\text{unrelax}} + O(f_{i\sigma}^3), \quad (7)$$

$$\Pi_{i\sigma}^{\text{r}} = \frac{1}{2} f_{i\sigma} (1 - f_{i\sigma}) \left. \frac{d^2 E^{\text{app}}}{df_{i\sigma}^2} \right|_{\text{relax}} + O(f_{i\sigma}^3) \quad (8)$$

$$\tilde{\varepsilon}^{-1} = 1 + f_{\text{Hxc}} \chi. \quad (9)$$

Here $\chi(\mathbf{r}, \mathbf{r}')$, $\tilde{\varepsilon}(\mathbf{r}, \mathbf{r}')$ and $f_{\text{Hxc}}^{\sigma\sigma'}(\mathbf{r}, \mathbf{r}') = \frac{\delta E_{\text{Hxc}}^{\text{app}}}{\delta \rho_{\sigma}(\mathbf{r}) \delta \rho_{\sigma'}(\mathbf{r}')}$ are the density-density response function, the microscopic dielectric matrix and the Hxc kernel, respectively, evaluated at the underlying approximate (app) functional.²⁹ The latter would be a standard density functional for KI and the PZ-SIC functional for KIPZ.³² While in the former case an efficient implemen-

tation based on the linear-response technique of density-functional perturbation theory can be used,²⁹ for the KIPZ functional a less elegant although straightforward finite difference approach is needed²⁸ since analytical derivatives and linear-response techniques for the PZ functional are not available in standard DFT codes.^{33,34}

Localization. The KC corrections in Eqs. (4) and (5) depend on each orbital density and the KC functional is therefore orbital-density dependent. At variance with density dependent functionals, orbital-density dependent functionals can break the invariance of the total energy against a unitary rotation of the occupied manifold.¹ For such functionals the *variational orbitals* that minimize the functional are different from the eigenstates or *canonical orbitals* that diagonalize the orbital-density dependent Hamiltonian (the Lagrange multiplier matrix), as discussed e.g in Refs. 21, 22 and Refs. 35–40 . Such duality is an important feature of any orbital-density dependent scheme. In general the variational orbitals exploit the additional freedom of unitary mixing to become localized^{21,41} (and similar to Wannier functions^{42–45}) in order to further lower the total energy.⁴⁶ On the other side the canonical orbitals and energies are the analogous of the single-particle KS-DFT or Hartree-Fock states and their energies are directly connected to those of Dyson orbitals and quasiparticle energies accessible, e.g., from photoemission experiments.^{22,35}

2.1 KC as a simplified electronic self-energy

To establish a connection with common electronic-structure approaches, we discuss here in some detail the actual form of the KC energy and potential corrections. To simplify the discussion we resort again to a Taylor expansion of the functionals in the orbital occupations. Following Ref. 29 we can write the fully relaxed KI and KIPZ corrections up to second order

¹ This is the case for the PZ-SIC and KIPZ functional, while for the KI functional at integer occupations the energy corrections vanish and the KI energy remains identical to the one of the underlying density functional.²¹

in the occupations as

$$\Pi_{i\sigma}^{\text{rKI}(2)} = \frac{1}{2}f_{i\sigma}(1-f_{i\sigma})\frac{d^2E^{\text{DFT}}}{df_{i\sigma}^2} = \frac{1}{2}f_{i\sigma}(1-f_{i\sigma})\langle n_{i\sigma}|\mathcal{F}_{\text{Hxc}}^{\sigma\sigma}|n_{i\sigma}\rangle, \quad (10)$$

$$\Pi_{i\sigma}^{\text{rKIPZ}(2)} = \Pi_{i\sigma}^{\text{rKI}(2)} - f_{i\sigma}E_{\text{Hxc}}[n_{i\sigma}] = \frac{1}{2}f_{i\sigma}(1-f_{i\sigma})\langle n_{i\sigma}|\mathcal{F}_{\text{Hxc}}^{\sigma\sigma}|n_{i\sigma}\rangle - f_{i\sigma}E_{\text{Hxc}}[n_{i\sigma}], \quad (11)$$

with $\mathcal{F}_{\text{Hxc}} = \tilde{\varepsilon}^{-1}f_{\text{Hxc}}$. The screened, additional, orbital dependent KC potential acting on the i -th electron is defined as the derivative of the relaxed KC energy $\Pi^{\text{KC}} = \sum_k \Pi_k^{\text{rKC}(2)} + O(f_k^3)$ with respect to the orbital density $\rho_{i\sigma}$. Adding also the xc contribution from the underlying DFT functional, the total orbital-density dependent xc potentials read, up to the second order:

$$v_{i\sigma,\text{xc}}^{\text{rKI}(2)}(\mathbf{r}) = v_{\sigma,\text{xc}}^{\text{DFT}}(\mathbf{r}) - \frac{1}{2}\langle n_{i\sigma}|\mathcal{F}_{\text{Hxc}}^{\sigma\sigma}|n_{i\sigma}\rangle + (1-f_{i\sigma})\int d\mathbf{r}'\mathcal{F}_{\text{Hxc}}^{\sigma\sigma}(\mathbf{r},\mathbf{r}')n_{i\sigma}(\mathbf{r}'), \quad (12)$$

$$v_{i\sigma,\text{xc}}^{\text{rKIPZ}(2)}(\mathbf{r}) = v_{i\sigma,\text{xc}}^{\text{rKI}(2)}(\mathbf{r}) - \left\{ E_{\text{Hxc}}[n_{i\sigma}] - \int d\mathbf{r}'v_{\sigma,\text{Hxc}}[n_{i\sigma}](\mathbf{r}')n_{i\sigma}(\mathbf{r}') + v_{\sigma,\text{Hxc}}[n_{i\sigma}](\mathbf{r}) \right\} \quad (13)$$

where the orbital dependent Hamiltonian is defined as $\hat{h}_{i\sigma}|\phi_{i\sigma}\rangle = \hat{h}_0|\phi_{i\sigma}\rangle + \hat{v}_{i\sigma,\text{xc}}^{\text{rKC}(2)}|\phi_{i\sigma}\rangle$, with $\hat{h}_0 = -\frac{1}{2}\nabla^2 + \hat{v}_{\text{ext}} + \hat{v}_{\text{H}}[\rho]$ the Hartree Hamiltonian. Note that in Eq. (12) we neglected the variation of $\mathcal{F}_{\text{Hxc}}^{\sigma\sigma}$ with respect to $\rho_{i\sigma}$ to stay within a second-order approximation.

In the absence of relaxation effects, i.e. assuming $\tilde{\varepsilon}^{-1} = 1$, and neglecting the xc contribution in the underlying DFT, i.e. using a Hartree-only functional, the KIPZ correction provides a good approximation of the non-local Hartree-Fock (HF) exchange operator when evaluated on a localized representation.²² In fact, the HF self energy Σ_{x} is given, in terms of the occupied single particle spin-orbitals, as

$$\Sigma_{\text{x}}(\mathbf{x},\mathbf{x}') = -\sum_{i\sigma}^{\text{occ}}\psi_{i\sigma}(\mathbf{x})\psi_{i\sigma}^*(\mathbf{x}')f_{\text{H}}(\mathbf{r},\mathbf{r}') \quad (14)$$

where $\psi_{i\sigma}(\mathbf{x})$ are spin-orbital wavefunctions and $\mathbf{x} = \{\mathbf{r},\xi\}$ is a composite variable for the spatial coordinate \mathbf{r} and the spin coordinate ξ . In the present work we neglect relativistic

effects such that $\psi_{i\sigma}(\mathbf{x}) = \phi_{i\sigma}(\mathbf{r})\pi_\sigma(\xi)$ factorizes in the product of a spatial function $\phi_{i\sigma}(\mathbf{r})$ and a spin function $\pi_\sigma(\xi)$ (see e.g. Ref. 47). Since Σ_x depends on the density matrix, it is invariant under unitary transformations of the occupied manifold and can be expressed on any equivalent representation of the occupied manifold. In a representation where the orbitals $\{\phi_{i\sigma}\}$ are as localized (non-overlapping) as possible, the off-diagonal contributions of the exchange operator can be neglected, and its matrix elements become:

$$\langle i\sigma | \Sigma_x | j\sigma' \rangle = - \sum_{k\sigma''}^{\text{occ}} \int d\mathbf{x} \psi_{i\sigma}^*(\mathbf{x}) \psi_{k\sigma''}(\mathbf{x}) \int d\mathbf{x}' \frac{\psi_{k\sigma''}^*(\mathbf{x}') \psi_{j\sigma'}(\mathbf{x}')}{|\mathbf{r} - \mathbf{r}'|} \quad (15)$$

$$\begin{aligned} &= - \sum_{k\sigma''}^{\text{occ}} \int d\mathbf{r} \phi_{i\sigma}^*(\mathbf{r}) \phi_{k\sigma''}(\mathbf{r}) \delta_{\sigma\sigma''} \int d\mathbf{r}' \frac{\phi_{k\sigma''}^*(\mathbf{r}') \phi_{j\sigma'}(\mathbf{r}')}{|\mathbf{r} - \mathbf{r}'|} \delta_{\sigma''\sigma'} \\ &\simeq - \langle \phi_{i\sigma} | v_{\text{H}}[n_{i\sigma}] | \phi_{i\sigma} \rangle \delta_{ij} \delta_{\sigma\sigma'}, \end{aligned} \quad (16)$$

where the Kronecker δ over the spin indices comes from the orthonormality of the spin functions. On the other hand, the matrix elements of the Hartree-only KIPZ potential without screening follow from Eq. (13), when any xc contribution is set to zero and $\tilde{\epsilon}^{-1} = 1$, and read

$$\langle i\sigma | v_{j\sigma',\text{xc}}^{\text{uKIPZ}(2)} | j\sigma' \rangle \simeq \delta_{ij} \delta_{\sigma\sigma'} \left\{ \left(\frac{1}{2} - f_{i\sigma} \right) \langle n_{i\sigma} | f_{\text{H}} | n_{i\sigma} \rangle - E_{\text{H}}[n_{i\sigma}] \right\} \quad (17)$$

that for occupied orbitals reduces to $-2E_{\text{H}}[n_{i\sigma}] \delta_{ij} \delta_{\sigma\sigma'} = - \langle \phi_{i\sigma} | v_{\text{H}}[n_{i\sigma}] | \phi_{i\sigma} \rangle \delta_{ij} \delta_{\sigma\sigma'}$.

If we now turn on screening effects at the Hartree level, the RPA (statically) screened interaction $W = \epsilon_{\text{RPA}}^{-1} f_{\text{H}}$ appears in Eq. (17), instead of the bare Coulomb kernel, and the KIPZ matrix elements become:

$$\langle i\sigma | v_{j\sigma',\text{xc}}^{\text{rKIPZ}(2)} | j\sigma' \rangle \simeq \delta_{ij} \delta_{\sigma\sigma'} \left\{ \left(\frac{1}{2} - f_{i\sigma} \right) \langle n_{i\sigma} | W | n_{i\sigma} \rangle - E_{\text{H}}[n_{i\sigma}] \right\}. \quad (18)$$

We now show that these matrix elements are similar to the static GW self-energy, known as

Coulomb-hole plus screened-exchange (COHSEX) self-energy:^{26,48,49}

$$\begin{aligned}
\Sigma_{\text{xc}}^{\text{COHSEX}} &= \Sigma_{\text{xc}}^{\text{SEX}} + \Sigma_{\text{xc}}^{\text{COH}}, \\
\Sigma_{\text{xc}}^{\text{SEX}}(\mathbf{x}, \mathbf{x}') &= - \sum_{k\sigma}^{\text{occ}} \psi_{k\sigma}(\mathbf{x}) \psi_{k\sigma}^*(\mathbf{x}') W(\mathbf{r}, \mathbf{r}'), \\
\Sigma_{\text{xc}}^{\text{COH}}(\mathbf{x}, \mathbf{x}') &= \frac{1}{2} \delta(\mathbf{x}, \mathbf{x}') [W(\mathbf{r}, \mathbf{r}') - f_{\text{H}}(\mathbf{r}, \mathbf{r}')].
\end{aligned} \tag{19}$$

Like the HF self-energy, also the COHSEX one depends only on the density-matrix (when keeping W constant, independent on the orbitals) and is then invariant under unitary rotations of the occupied manifold. Rewriting the δ function using a completeness relation, $\delta(\mathbf{x}, \mathbf{x}') = \sum_{k\sigma} \psi_{k\sigma}(\mathbf{x}) \psi_{k\sigma}^*(\mathbf{x}')$, and assuming again to work on a localized representation of the manifold to neglect off-diagonal contributions, the COHSEX matrix elements become (see SI for a detailed derivation):

$$\langle i\sigma | \Sigma_{\text{xc}}^{\text{COHSEX}} | j\sigma' \rangle \simeq \delta_{ij} \delta_{\sigma\sigma'} \left\{ \left(\frac{1}{2} - f_{i\sigma} \right) \langle n_{i\sigma} | W | n_{i\sigma} \rangle - \frac{1}{2} \langle n_{i\sigma} | f_{\text{H}} | n_{i\sigma} \rangle \right\}. \tag{20}$$

The second term in the curly brackets is nothing but the self-Hartree of the orbital $i\sigma$, and the equation above matches exactly with Eq. (18). As already stated, so far we have only considered the Hartree and screening contributions to the potentials. On one side, this derivation highlights the role of the KC potentials as local and orbital dependent approximation to non-local self energies. On the other side, when a more advanced DFT functional is used as a starting point, also the xc potential and f_{xc} kernel play a role.

The inclusion of f_{xc} transforms the test charge-test charge (RPA) dielectric function in the test charge-test electron response.^{5,50-52} The electrons that participate to the screening have now an approximate xc-hole surrounding them and the potential induced by the additional electron or hole includes xc-interactions and not only the classical Hartree term; the induced charge-density of the interacting system can be written^{53,54} as the charge density response of the auxiliary KS (non-interacting) system to an effective perturbation, i.e. $\delta\rho = \chi_0 \delta V_{\text{tot}}$

where χ_0 is the KS density-density response function. The effective potential δV_{tot} includes not only the external perturbation but also the self-consistent variation of the Hxc potential induced by the changes in the charge density, i.e. $\delta V_{\text{tot}} = \delta V_{\text{ext}} + \delta V_{\text{Hxc}}$. The inclusion of xc effects at the DFT level makes the link to a corresponding self-energy less trivial. However, we argue that a screened KIPZ Hamiltonian built on a local or semi-local density functional may be a good approximation to a more sophisticated self-energy operator where also simple (DFT based) vertex corrections are included (see discussion below).

Following Refs. 55 and 51 a zero-order approximation for the self-energy can be defined using the DFT xc potential,⁵⁶ i.e. $\Sigma_{\text{xc}}(1, 2) = \delta(1, 2)V_{\text{xc}}(1)$ [we used the compact notation $1=(\mathbf{r}_1, t_1)$]; the first iteration of the Hedin's equation²⁶ leads to a GW Γ approximation of the self energy that has an expression very similar to the RPA one, i.e. $\Sigma(1, 2) = iG(1, 2)\tilde{W}(1, 2)$, but with a screened interaction that accounts for xc effects beyond the classical Hartree one: $\tilde{W} = \tilde{\epsilon}^{-1}f_{\text{H}} = f_{\text{H}}[1 - \chi_0 f_{\text{Hxc}}]^{-1}$. Within this approximation Eq. (20) gets modified since now W is replaced by \tilde{W} . The bare Coulomb interaction is now screened by the test charge-test electron response function $\tilde{\epsilon}^{-1}$, which is the one appearing also in the definition of the KC screening parameters, Eqs. (6) and (9). Still a direct comparison of Eq. (20), including the improved screened interaction \tilde{W} , with the full KIPZ matrix elements

$$\langle i\sigma | v_{j\sigma', \text{xc}}^{\text{rKIPZ}(2)} | j\sigma' \rangle \simeq \delta_{ij} \delta_{\sigma\sigma'} \left\{ \langle \phi_{i\sigma} | v_{\sigma, \text{xc}}^{\text{DFT}} | \phi_{i\sigma} \rangle + \left(\frac{1}{2} - f_{i\sigma} \right) \langle n_{i\sigma} | \mathcal{F}_{\text{Hxc}}^{\sigma\sigma} | n_{i\sigma} \rangle - E_{\text{Hxc}}[n_{i\sigma}] \right\} \quad (21)$$

is not trivial, and is hindered by the presence of the xc energy and potential of the underlying DFT functional. Nevertheless, the similarity between the two approaches is apparent also in this case, and highlights the physical ingredients present in the KIPZ orbital-dependent potentials.

3 Computational Details

In the next Sections we provide numerical results from KC calculations on the GW100 test set. This set has been introduced²⁷ to benchmark and validate different GW implementations and is made of 100 small closed-shell molecules with diverse chemical bonding. For consistency we adopt the same molecular geometries provided in the original work. In our analysis we focus on the first ionization potential (IP) for which accurate CCSD(T) results are available; for a subset of molecules we also look at transitions from deeper valence states for which a comparison with experimental data (photoemission spectroscopy) is available.

Standard DFT calculations presented here have been performed using the PWSCF code in the QUANTUM ESPRESSO^{33,57} distribution. Extensive convergence tests on the energy cut-off for the plane-wave expansion, as well on the size of the supercell have been performed to ensure a converged value of the first IP within 10 meV. The supercell size convergence has been facilitated thanks to the use of reciprocal-space counter-charge corrections.^{58,59} The electron-ion interactions have been modeled using Optimized Norm-Conserving Vanderbilt (ONCV) pseudopotentials⁶⁰ as developed by Schlipf and Gygi.^{61,62} The KC calculations have been performed using a modified version of the QUANTUM ESPRESSO CP code and adopt the Perdew, Burke and Ernzerhof (PBE) exchange-correlation functional⁶³ as the underlying base functional. The minimization of the orbital-density dependent functionals has been done on the space of complex-valued wavefunctions; the strategy we use for the optimization follows the ensemble-DFT algorithm⁶⁴ and consist of two nested loops;⁶⁵ in the inner loop we search for the optimal unitary transformation that minimizes the orbital-density dependent part of the energy functional at fixed manifold; in the outer loop a standard conjugate-gradients algorithm is used to optimize the manifold. The orbital-density dependent screening coefficients have been computed according to Eq. (6) using the linear-response scheme described in Ref. 29; for the case of KIPZ, where this scheme is not applicable due the lack of an implementation of linear-response analytical derivatives for the PZ-SIC functional, we resort to the finite difference approach outlined in Ref. 28.

The theoretical IPs are defined as minus the eigenvalue of the corresponding molecular orbital⁶⁶ for all the theoretical methods reported, except for Δ SCF. In the latter case only the first IP has been computed, defined as the energy difference between the neutral molecule and its cation.

4 Results

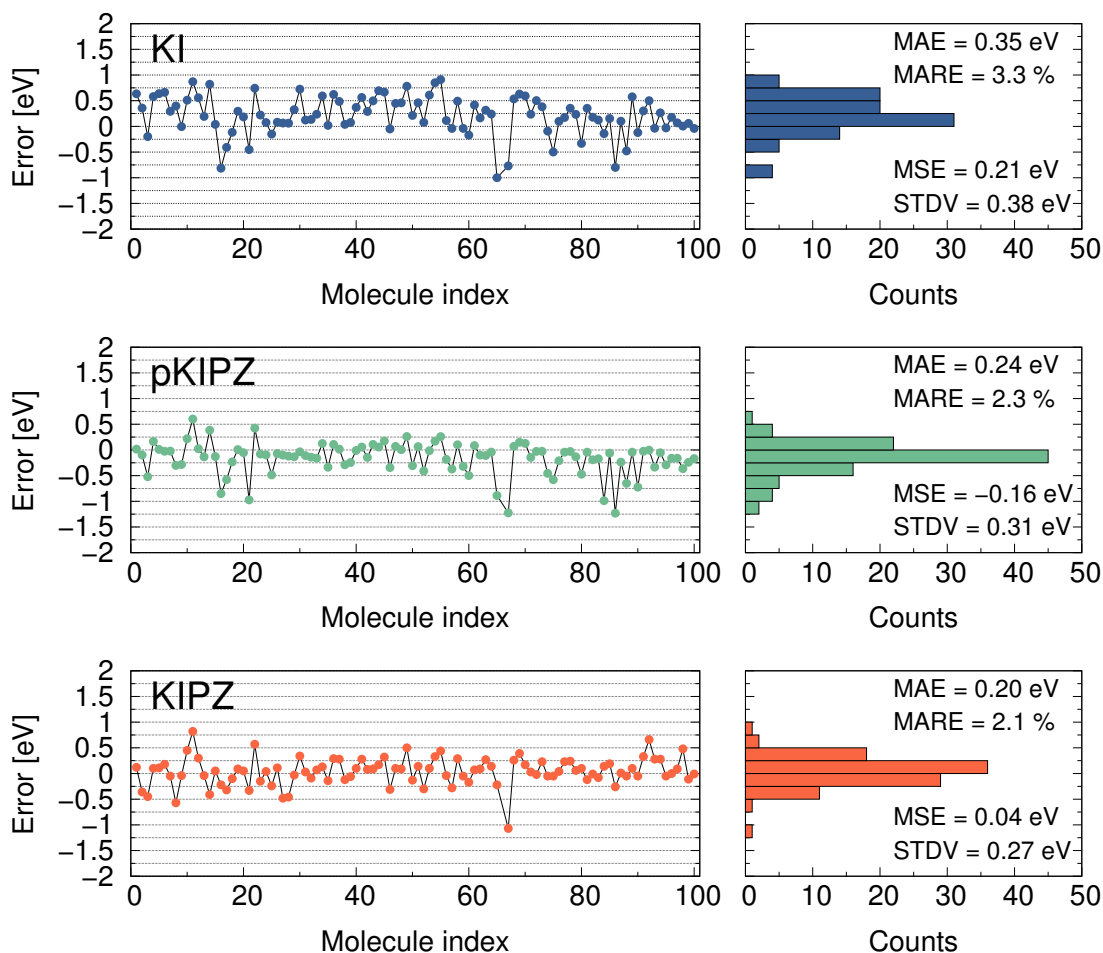


Figure 1: Errors (left panels) on the first ionization potentials with respect to CCSD(T) Δ SCF results⁶⁷ and their distributions (right panel) at different levels of the theory. Top panel KI, central panel perturbative KIPZ and bottom panel full KIPZ (see text for details).

4.1 First ionization potential

In this Section we analyze the average performance of the KC functionals described in Sec. 2. To begin with, we focus on the first ionization potential (IP), for which accurate quantum-chemistry calculations (such as, e.g., Δ SCF CCSD(T) at the def2-TZVPP level) are available in the literature.⁶⁷ Comparison against high-accuracy methods allows one to remove the experimental uncertainties and strictly focus on the failures of the theory. To quantify the agreement with respect to the CCSD(T) reference we look at the Mean Absolute Error (MAE), the Mean Absolute Relative Error (MARE), the Mean Signed Error (MSE), and the Standard Deviation (STDV), defined as

$$\begin{aligned}
 \text{MAE} &= \frac{1}{N} \sum_{i=1}^N |\Delta\text{IP}_i| \\
 \text{MARE} &= \frac{1}{N} \sum_{i=1}^N |\Delta\text{IP}_i/\text{IP}_i^{\text{R}}| \\
 \text{MSE} &= \frac{1}{N} \sum_{i=1}^N \Delta\text{IP}_i \\
 \text{STDV} &= \sqrt{\frac{1}{N} \sum_{i=1}^N (\Delta\text{IP}_i - \text{MSE})^2}
 \end{aligned} \tag{22}$$

with $\Delta\text{IP} = \text{IP} - \text{IP}^{\text{R}}$ the error in the ionization potential IP with respect to the reference [CCSD(T)] value IP^{R} .

In Fig. 1 we present the results for the first ionization potentials calculated within the KI and KIPZ functionals (top and bottom panels, respectively). We also report results for perturbative KIPZ calculations (pKIPZ in the plots and tables, middle panel) where the KIPZ correction is computed on top of the KI minimizing orbitals, thus neglecting self-consistency effects at the KIPZ level. We recall here that the KI total energy at integer occupation numbers coincides with that of the underlying density functional and thus KI preserves its unitary invariance under rotation of the manifold. As already discussed in previous works^{21,29} we choose a specific manifold by introducing an infinitesimally small PZ-

SIC contribution to the KI energy. This allows us to (1) unambiguously define the manifold, since the small PZ-SIC term breaks the unitary invariance, and to (2) localize the orbitals without modifying the ground state energy.

The performance of these three KC functionals is summarized in the right panels of Fig. 1. Our calculations find that KI slightly overestimates the ionization potential by 0.21 eV, on average (MSE). Simply applying the KIPZ correction in a perturbative way significantly improves the results reducing the MAE by 0.11 eV and narrowing the distribution of the error. A MSE of -0.16 eV indicates an underestimation of the IP on average, with an opposite trend with respect to the KI calculation. A full KIPZ calculation reduces further both the MAE (0.20 eV) and the STDV (0.27 eV), the error distribution being nicely centered around zero with a MSE of 0.04 eV. Notwithstanding the further improvement obtained within KIPZ, we note that the largest change happens when passing from KI to pKIPZ. This seems to suggest that the main reason for the improvement is in the KIPZ Hamiltonian and only secondarily in the self-consistency effects (changes in the orbitals and orbital densities). Indeed, the definition of the KI functional can be thought of as the limit of the full KIPZ functional when the PZ-SIC contribution is sent to zero²¹ (see Eq. 5), and thus further justifies the use of the KI manifold as the starting point for the perturbative KIPZ calculation.

In Fig. 2 we compare KC functionals with other electronic structure methods characterized by different level of complexity: the LDA-1/2 approach,⁷² a purely KS scheme based on a local potential; Hartree-Fock (HF) and dielectric dependent hybrid (DDH) functionals,⁷³⁻⁷⁵ accounting for the non-locality of the potential; and various GW schemes ranging from perturbative G_0W_0 to fully self-consistent GW, taking also into account the (dynamical) screening in the effective single particle potential (self-energy). In terms of complexity, KC functionals, with their local but orbital-dependent potentials, stand in between LDA-1/2 and the hybrid functionals. It is remarkable then that the accuracy they achieve is comparable or actually superior to that of more sophisticated electronic structure approaches with the smallest error compared to CCSD(T).

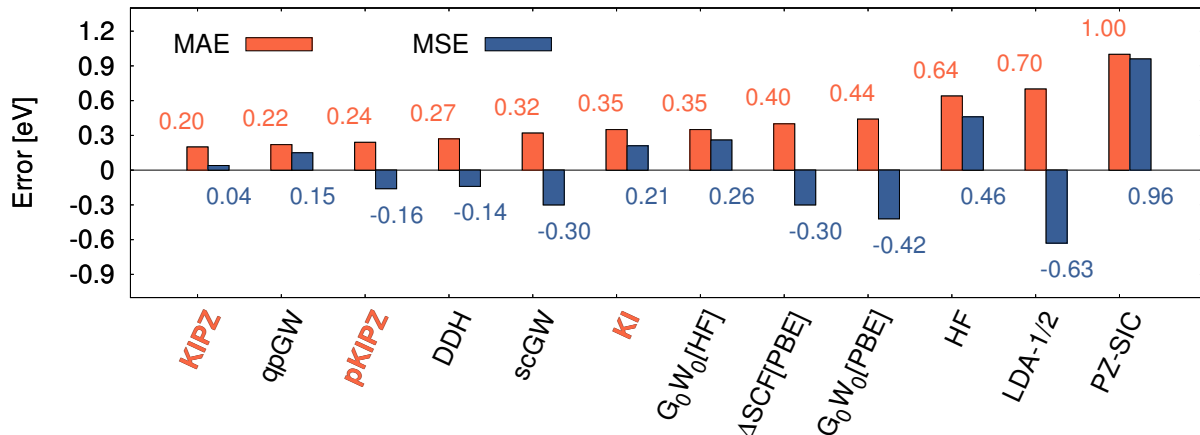


Figure 2: Comparison of the average performance of the KC functionals with other electronic structure methods. HF and LDA-1/2 results from Ref. 68, DDH from Ref. 69, G₀W₀[PBE] from Ref. 70 and G₀W₀[HF], scGW and qpGW from Ref. 71. Red labels on the horizontal axis are used to highlight KC functionals.

It is fair to say that although the KC potentials are local, the computation of all the ingredients needed, and in particular of the screening coefficients, requires additional effort. This is apparent from Eq. (6), where screening is defined as an orbital-dependent average of the static DFT dielectric matrix. This resonates with DDH functionals, where the mixing parameter is obtained from a screened-exchange calculation and thus ultimately requires the knowledge of the (static) RPA dielectric matrix. However, it is important to stress that the scheme we use to compute the $\{\alpha_{i\sigma}\}$ ²⁹ does not require to build up the whole dielectric matrix [neither in a PW basis (as done in standard implementations) nor in any other optimal basis (as done for DDH^{69,75})]; we instead compute “on the fly” the action of the dielectric matrix on the orbital density that we are considering. The evaluation of each screening coefficient requires thus a linear-response calculation that scales roughly as an electronic self-consistent DFT calculation. Moreover, since the variational orbitals are Wannier-like, they form groups with very similar screening coefficients; although not exploited here, this feature would allow one to greatly reduce the number of independent linear response calculations^{28,29} and speed up and/or streamline the calculations.

4.2 Deeper valence states

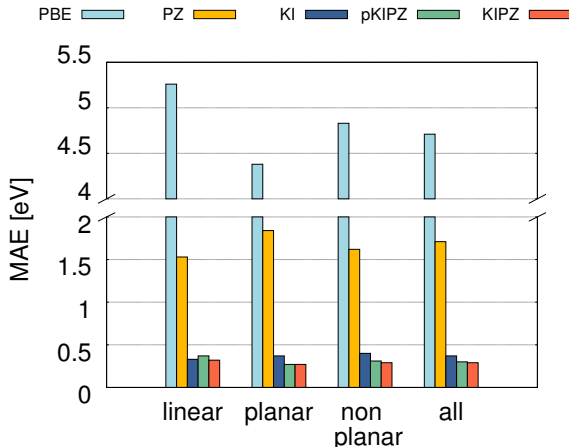


Figure 3: MAE on the deeper valence state IPs with respect to experimental values for different functionals. The average is first performed separately on 18 IPs from a subset of linear molecules (N_2 , F_2 , HF, CO, HCN, C_2H_2), on 38 IPs from a subset of planar molecules (H_2O , C_2H_4 , O_3 , HCOOH, benzene and pyridine) and on 21 IPs from a subset of non-planar molecules (NH_3 , PH_3 , C_2H_6 , CF_4 , CCl_4), and then on the 77 transitions all together. The complete list of vertical ionization potentials considered is given in SI.

In this Section we report results concerning the use of Koopmans functionals to evaluate low-lying single particle energies. The linearity condition typical of all the KC flavors applies to the entire electronic manifold (and not just to the highest occupied orbital, as in exact DFT), and one thus expects meaningful corrections also for states different from the HOMO. We considered 77 vertical ionization potentials from a subset of the molecules studied, for which experimental results are available in Refs. 8 and 76 (and references therein). We group the molecules according to their chemical and structural properties: the first group comprises 6 linear molecules including simple dimers (N_2 and F_2), polar molecules (HF and CO), and two molecules with a strong bond, i.e. hydrogen cyanide (C-N triple bond) and the simplest alkyne C_2H_2 (C-C triple bond). The second group is made by 6 planar molecules (O_3 , H_2O , HCOOH, C_2H_4 , benzene and pyridine) of increasing size, with benzene and pyridine representative for aromatic, organic molecules. The last group comprises 6 small non-planar molecules (NH_3 , PH_3 , C_2H_6 , CF_4 , CCl_4). We mainly consider transitions with binding energies smaller than 21.2 eV, i.e. accessible via He(I) ultraviolet photoemission

Table 1: MAE and MSE from experiments on the deeper valence state IPs from the subset of 18 molecules considered in Sec. 4.2 and for different functionals. The average is first performed separately on the 18 IPs from the linear molecules, on the 38 IPs from the planar molecules, and on the 21 IPs from the non-planar molecules, and then on all the 77 transitions. The MAE and MSE only on the 18 first IPs is also given in the last two lines.

Type of Molecule		PBE	PZ-SIC	KI	pKIPZ	KIPZ
Linear	MAE	5.26	1.53	0.33	0.37	0.32
	MSE	-5.26	1.47	0.08	-0.21	0.06
Planar	MAE	4.38	1.84	0.37	0.27	0.27
	MSE	-4.38	1.84	0.22	-0.06	0.06
Non-planar	MAE	4.83	1.62	0.40	0.31	0.29
	MSE	-4.83	1.62	0.11	-0.08	0.08
All IPs (77)	MAE	4.71	1.71	0.37	0.30	0.29
	MSE	-4.71	1.69	0.16	-0.10	0.06
First IPs (18)	MAE	4.62	1.21	0.37	0.32	0.23
	MSE	-4.62	1.20	0.22	-0.17	0.06

spectroscopy, with few exceptions where higher binding-energy transitions are also included (see SI for the complete list of vertical ionization potentials considered).

In Fig. 3 and Tab. 1 we show the average performance of PBE, PZ-SIC and the KC functionals with respect to experimental results. For the IPs considered we observe the same trend found for the case of the HOMO when moving from standard density functionals to PZ-SIC and eventually to KC; the PBE eigenvalues greatly underestimate the experimental values while PZ-SIC tends to overestimate transition energies. All the KC flavors show a more balanced performance with pKIPZ and KIPZ having very similar MAE and MSE. Most importantly, we do not observe any significant difference in the average performance when deeper states are concerned. This is clear from the comparison of the last two lines in Tab. 1 where the average over all transitions and the average over only the first ionization energies are listed. Only for PZ-SIC an increase of the errors by ~ 0.5 eV is observed when deeper states are included in the average; for all the KC functionals very small changes are observed (0.00 eV, -0.02 eV, +0.06 eV in the MAE for KI, pKIPZ and KIPZ, respectively), highlighting

the predictive capabilities of Koopmans-compliant functional also for states different from the HOMO.

5 Conclusions

In conclusion, we have investigated in detail Koopmans-compliant functionals highlighting similarity and differences with respect to other well established electronic structure methods, and tested the full GW100 protocol. We show that the local and orbital-density dependent potentials typical of KC functionals can be thought of as a simplified yet accurate approximation to the self-energy operator beyond the GW approximation. We stressed once again the importance of the local nature of the variational orbitals that ultimately is responsible for the possibility to map the non-local self-energy operator into local but orbital dependent potentials. We ascribe the remarkably good performance of KC functionals (and in particular of KIPZ) to the inclusion of local vertex corrections which allow for an improved description of the screening processes and self-energies beyond the RPA approximation, typical of standard GW approaches. This theoretical analysis is supported by the numerical calculations of ionization potentials for the large (and standardized) GW100 set of molecules. The KIPZ functionals show remarkably good performance with a MAE of 0.20 eV, significantly better than all standard perturbative G_0W_0 results and in line with GW calculations when some sort of self-consistency is considered. On the basis of the theoretical analysis presented here we argue that the inclusion of vertex corrections may be important to further close the gap between Green's function methods results and CCCSD(T). In the KC functionals this is done at the DFT level with a local vertex function. When deeper valence states are concerned, no significant change in the average performance of the KC functionals is observed, highlighting the effectiveness of the orbital-density dependent potentials in accurately describing the whole electronic structure manifold and not just the first ionization potential.

Acknowledgement

This research was supported by the Swiss National Science Foundation (SNSF), through Grant No. 200021-179139, and its National Centre of Competence in Research (NCCR) MARVEL. We acknowledge the computing center of EPFL for high performance computing resources.

Supporting Information Available

The following files are available free of charge. The Supporting Information contains details on the derivation of Eq. 20 in Sec. 2.1; the complete list of the first ionization potentials for the entire set of 100 molecule (Tab. SI-1) and the list of 77 deeper vertical ionization potentials (Tabs. SI-2, SI-3 and SI-4) for the subset of molecules considered in Sec 4.2.

References

- (1) Yu, L.; Zunger, A. Identification of Potential Photovoltaic Absorbers Based on First-Principles Spectroscopic Screening of Materials. *Phys. Rev. Lett.* **2012**, *108*, 068701.
- (2) E. Castelli, I.; Olsen, T.; Datta, S.; D. Landis, D.; Dahl, S.; S. Thygesen, K.; W. Jacobsen, K. Computational screening of perovskite metal oxides for optimal solar light capture. *En. Environ. Sci.* **2012**, *5*, 5814–5819.
- (3) Jain, A.; Shin, Y.; Persson, K. A. Computational predictions of energy materials using density functional theory. *Nature Reviews Materials* **2016**, *1*, 15004.
- (4) Pham, T. A.; Govoni, M.; Seidel, R.; Bradforth, S. E.; Schwegler, E.; Galli, G. Electronic structure of aqueous solutions: Bridging the gap between theory and experiments. *Sci. Adv.* **2017**, *3*, e1603210.

- (5) Onida, G.; Reining, L.; Rubio, A. Electronic excitations: density-functional versus many-body Green's-function approaches. *Rev. Mod. Phys.* **2002**, *74*, 601–659.
- (6) Perdew, J. P.; Parr, R. G.; Levy, M.; Balduz, J. L. Density-Functional Theory for Fractional Particle Number: Derivative Discontinuities of the Energy. *Phys. Rev. Lett.* **1982**, *49*, 1691–1694.
- (7) Almbladh, C.-O.; von Barth, U. Exact results for the charge and spin densities, exchange-correlation potentials, and density-functional eigenvalues. *Phys. Rev. B* **1985**, *31*, 3231–3244.
- (8) Chong, D. P.; Gritsenko, O. V.; Baerends, E. J. Interpretation of the Kohn–Sham orbital energies as approximate vertical ionization potentials. *J. Chem. Phys.* **2002**, *116*, 1760–1772.
- (9) Cococcioni, M.; de Gironcoli, S. Linear response approach to the calculation of the effective interaction parameters in the $\text{LDA}+\text{U}$ method. *Phys. Rev. B* **2005**, *71*, 035105.
- (10) Kulik, H. J.; Cococcioni, M.; Scherlis, D. A.; Marzari, N. Density Functional Theory in Transition-Metal Chemistry: A Self-Consistent Hubbard U Approach. *Phys. Rev. Lett.* **2006**, *97*, 103001.
- (11) Dabo, I.; Cococcioni, M.; Marzari, N. Non-Koopmans Corrections in Density-functional Theory: Self-interaction Revisited. *arXiv:0901.2637 [cond-mat]* **2009**, arXiv: 0901.2637.
- (12) Dabo, I.; Ferretti, A.; Poilvert, N.; Li, Y.; Marzari, N.; Cococcioni, M. Koopmans' condition for density-functional theory. *Phys. Rev. B* **2010**, *82*, 115121.
- (13) Stein, T.; Eisenberg, H.; Kronik, L.; Baer, R. Fundamental Gaps in Finite Systems

- from Eigenvalues of a Generalized Kohn-Sham Method. *Phys. Rev. Lett.* **2010**, *105*, 266802.
- (14) Zheng, X.; Cohen, A. J.; Mori-Sánchez, P.; Hu, X.; Yang, W. Improving Band Gap Prediction in Density Functional Theory from Molecules to Solids. *Phys. Rev. Lett.* **2011**, *107*, 026403.
- (15) Kraisler, E.; Kronik, L. Piecewise Linearity of Approximate Density Functionals Revisited: Implications for Frontier Orbital Energies. *Phys. Rev. Lett.* **2013**, *110*, 126403.
- (16) Görling, A. Exchange-correlation potentials with proper discontinuities for physically meaningful Kohn-Sham eigenvalues and band structures. *Phys. Rev. B* **2015**, *91*, 245120.
- (17) Li, C.; Zheng, X.; Cohen, A. J.; Mori-Sánchez, P.; Yang, W. Local Scaling Correction for Reducing Delocalization Error in Density Functional Approximations. *Phys. Rev. Lett.* **2015**, *114*, 053001.
- (18) Kronik, L.; Stein, T.; Refaely-Abramson, S.; Baer, R. Excitation Gaps of Finite-Sized Systems from Optimally Tuned Range-Separated Hybrid Functionals. *J. Chem. Theory Comput.* **2012**, *8*, 1515–1531.
- (19) Refaely-Abramson, S.; Sharifzadeh, S.; Govind, N.; Autschbach, J.; Neaton, J. B.; Baer, R.; Kronik, L. Quasiparticle Spectra from a Nonempirical Optimally Tuned Range-Separated Hybrid Density Functional. *Phys. Rev. Lett.* **2012**, *109*, 226405.
- (20) Li, C.; Zheng, X.; Su, N. Q.; Yang, W. Localized orbital scaling correction for systematic elimination of delocalization error in density functional approximations. *Natl. Sci. Rev.* **2018**,
- (21) Borghi, G.; Ferretti, A.; Nguyen, N. L.; Dabo, I.; Marzari, N. Koopmans-compliant

- functionals and their performance against reference molecular data. *Phys. Rev. B* **2014**, *90*, 075135.
- (22) Ferretti, A.; Dabo, I.; Cococcioni, M.; Marzari, N. Bridging density-functional and many-body perturbation theory: Orbital-density dependence in electronic-structure functionals. *Phys. Rev. B* **2014**, *89*, 195134.
- (23) Gatti, M.; Olevano, V.; Reining, L.; Tokatly, I. V. Transforming Nonlocality into a Frequency Dependence: A Shortcut to Spectroscopy. *Phys. Rev. Lett.* **2007**, *99*, 057401.
- (24) Vanzini, M.; Reining, L.; Gatti, M. Dynamical local connector approximation for electron addition and removal spectra. *arXiv:1708.02450 [cond-mat]* **2017**, arXiv:1708.02450.
- (25) Vanzini, M.; Reining, L.; Gatti, M. Spectroscopy of the Hubbard dimer: the spectral potential. *Eur. Phys. J. B* **2018**, *91*, 192.
- (26) Hedin, L. New Method for Calculating the One-Particle Green's Function with Application to the Electron-Gas Problem. *Phys. Rev.* **1965**, *139*, A796–A823.
- (27) van Setten, M. J.; Caruso, F.; Sharifzadeh, S.; Ren, X.; Scheffler, M.; Liu, F.; Lischner, J.; Lin, L.; Deslippe, J. R.; Louie, S. G.; Yang, C.; Weigend, F.; Neaton, J. B.; Evers, F.; Rinke, P. GW100: Benchmarking G0W0 for Molecular Systems. *J. Chem. Theory Comput.* **2015**, *11*, 5665–5687.
- (28) Nguyen, N. L.; Colonna, N.; Ferretti, A.; Marzari, N. Koopmans-Compliant Spectral Functionals for Extended Systems. *Phys. Rev. X* **2018**, *8*, 021051.
- (29) Colonna, N.; Nguyen, N. L.; Ferretti, A.; Marzari, N. Screening in Orbital-Density-Dependent Functionals. *J. Chem. Theory Comput.* **2018**, *14*, 2549–2557.
- (30) Perdew, J. P.; Zunger, A. Self-interaction correction to density-functional approximations for many-electron systems. *Phys. Rev. B* **1981**, *23*, 5048–5079.

- (31) Cohen, A. J.; Mori-Sánchez, P.; Yang, W. Insights into Current Limitations of Density Functional Theory. *Science* **2008**, *321*, 792–794.
- (32) Actually for the case of KIPZ one would need the second derivative of the PZ-SIC functional with respect to the orbital density, rather than the total density.
- (33) Giannozzi, P. et al. Advanced capabilities for materials modelling with Q uantum ESPRESSO. *J. Phys.: Condens. Matter* **2017**, *29*, 465901.
- (34) Gonze, X. et al. Recent developments in the ABINIT software package. *Computer Physics Communications* **2016**, *205*, 106–131.
- (35) Nguyen, N. L.; Borghi, G.; Ferretti, A.; Dabo, I.; Marzari, N. First-Principles Photoemission Spectroscopy and Orbital Tomography in Molecules from Koopmans-Compliant Functionals. *Phys. Rev. Lett.* **2015**, *114*, 166405.
- (36) Lehtola, S.; Jónsson, H. Variational, Self-Consistent Implementation of the Perdew–Zunger Self-Interaction Correction with Complex Optimal Orbitals. *J. Chem. Theory Comput.* **2014**, *10*, 5324–5337.
- (37) Vydrov, O. A.; Scuseria, G. E.; Perdew, J. P. Tests of functionals for systems with fractional electron number. *J. Chem. Phys.* **2007**, *126*, 154109.
- (38) Pederson, M. R.; Heaton, R. A.; Lin, C. C. Local-density Hartree–Fock theory of electronic states of molecules with self-interaction correction. *J. Chem. Phys.* **1984**, *80*, 1972–1975.
- (39) Stengel, M.; Spaldin, N. A. Self-interaction correction with Wannier functions. *Phys. Rev. B* **2008**, *77*, 155106.
- (40) Hofmann, D.; Klüpfel, S.; Klüpfel, P.; Kümmel, S. Using complex degrees of freedom in the Kohn-Sham self-interaction correction. *Phys. Rev. A* **2012**, *85*, 062514.

- (41) Pederson, M. R.; Lin, C. C. Localized and canonical atomic orbitals in self-interaction corrected local density functional approximation. *J. Chem. Phys.* **1988**, *88*, 1807–1817.
- (42) Edmiston, C.; Ruedenberg, K. Localized Atomic and Molecular Orbitals. *Rev. Mod. Phys.* **1963**, *35*, 457–464.
- (43) Boys, S. F. Construction of Some Molecular Orbitals to Be Approximately Invariant for Changes from One Molecule to Another. *Rev. Mod. Phys.* **1960**, *32*, 296–299.
- (44) Foster, J. M.; Boys, S. F. Canonical Configurational Interaction Procedure. *Rev. Mod. Phys.* **1960**, *32*, 300–302.
- (45) Marzari, N.; Mostofi, A. A.; Yates, J. R.; Souza, I.; Vanderbilt, D. Maximally localized Wannier functions: Theory and applications. *Rev. Mod. Phys.* **2012**, *84*, 1419–1475.
- (46) KI functional at integer occupations is invariant under unitary rotations; a representation is chosen²¹ by taking it as the limit of the KIPZ functional when the PZ correction tends to zero (as discussed in Section 4.1).
- (47) Szabo, A.; Ostlund, N. S. *Modern Quantum Chemistry: Introduction to Advanced Electronic Structure Theory*, revised. edizione ed.; Dover Pubns: Mineola, N.Y., 1996.
- (48) Gygi, F.; Baldereschi, A. Quasiparticle energies in semiconductors: Self-energy correction to the local-density approximation. *Phys. Rev. Lett.* **1989**, *62*, 2160–2163.
- (49) Kang, W.; Hybertsen, M. S. Enhanced static approximation to the electron self-energy operator for efficient calculation of quasiparticle energies. *Phys. Rev. B* **2010**, *82*, 195108.
- (50) Hybertsen, M. S.; Louie, S. G. Ab initio static dielectric matrices from the density-functional approach. I. Formulation and application to semiconductors and insulators. *Phys. Rev. B* **1987**, *35*, 5585–5601.

- (51) Del Sole, R.; Reining, L.; Godby, R. W. $GW\Gamma$ approximation for electron self-energies in semiconductors and insulators. *Phys. Rev. B* **1994**, *49*, 8024–8028.
- (52) Bruneval, F.; Sottile, F.; Olevano, V.; Del Sole, R.; Reining, L. Many-Body Perturbation Theory Using the Density-Functional Concept: Beyond the GW Approximation. *Phys. Rev. Lett.* **2005**, *94*, 186402.
- (53) Gross, E. K. U.; Kohn, W. Local density-functional theory of frequency-dependent linear response. *Phys. Rev. Lett.* **1985**, *55*, 2850–2852.
- (54) Petersilka, M.; Gossmann, U. J.; Gross, E. K. U. Excitation Energies from Time-Dependent Density-Functional Theory. *Phys. Rev. Lett.* **1996**, *76*, 1212–1215.
- (55) Hybertsen, M. S.; Louie, S. G. Electron correlation in semiconductors and insulators: Band gaps and quasiparticle energies. *Phys. Rev. B* **1986**, *34*, 5390–5413.
- (56) A rigorous justification for such a starting point is provided by the fact that the exact KS exchange-correlation potential is the variationally best local approximation to the exchange-correlation self-energy[?] .
- (57) Giannozzi, P. et al. QUANTUM ESPRESSO: a modular and open-source software project for quantum simulations of materials. *J. Phys.: Conden. Matter* **2009**, *21*, 395502.
- (58) Li, Y.; Dabo, I. Electronic levels and electrical response of periodic molecular structures from plane-wave orbital-dependent calculations. *Phys. Rev. B* **2011**, *84*, 155127.
- (59) Martyna, G. J.; Tuckerman, M. E. A reciprocal space based method for treating long range interactions in ab initio and force-field-based calculations in clusters. *J. Chem. Phys.* **1999**, *110*, 2810–2821.
- (60) Hamann, D. R. Optimized norm-conserving Vanderbilt pseudopotentials. *Phys. Rev. B* **2013**, *88*, 085117.

- (61) Schlipf, M.; Gygi, F. Optimization algorithm for the generation of ONCV pseudopotentials. *Comput. Phys. Commun.* **2015**, *196*, 36–44.
- (62) SG15 ONCV Potentials. 2017; http://www.quantum-simulation.org/potentials/sg15_oncv/.
- (63) Perdew, J. P.; Burke, K.; Ernzerhof, M. Generalized Gradient Approximation Made Simple. *Phys. Rev. Lett.* **1996**, *77*, 3865–3868.
- (64) Marzari, N.; Vanderbilt, D.; Payne, M. C. Ensemble Density-Functional Theory for Ab Initio Molecular Dynamics of Metals and Finite-Temperature Insulators. *Phys. Rev. Lett.* **1997**, *79*, 1337–1340.
- (65) Borghi, G.; Park, C.-H.; Nguyen, N. L.; Ferretti, A.; Marzari, N. Variational minimization of orbital-density-dependent functionals. *Phys. Rev. B* **2015**, *91*, 155112.
- (66) A direct identification of $-\varepsilon_i$ with the IP is possible thanks to the use of counter-charge corrections that enforce the correct asymptotic limit of the potential, that is $v(\mathbf{r}) = 0$ (vacuum level) when $\mathbf{r} \rightarrow \infty$ (i.e. far from the system).
- (67) Krause, K.; Harding, M. E.; Klopper, W. Coupled-cluster reference values for the GW27 and GW100 test sets for the assessment of GW methods. *Molecular Physics* **2015**, *113*, 1952–1960.
- (68) Pela, R. R.; Gulans, A.; Draxl, C. The LDA-1/2 method applied to atoms and molecules. *arXiv:1805.09705 [cond-mat, physics:physics]* **2018**, arXiv: 1805.09705.
- (69) Brawand, N. P.; Govoni, M.; Vörös, M.; Galli, G. Performance and Self-Consistency of the Generalized Dielectric Dependent Hybrid Functional. *J. Chem. Theory Comput.* **2017**,
- (70) Govoni, M.; Galli, G. GW100: Comparison of Methods and Accuracy of Results Obtained with the WEST Code. *J. Chem. Theory Comput.* **2018**, *14*, 1895–1909.

- (71) Caruso, F.; Dauth, M.; van Setten, M. J.; Rinke, P. Benchmark of GW Approaches for the GW100 Test Set. *J. Chem. Theory Comput.* **2016**, *12*, 5076–5087.
- (72) Ferreira, L. G.; Marques, M.; Teles, L. K. Approximation to density functional theory for the calculation of band gaps of semiconductors. *Phys. Rev. B* **2008**, *78*, 125116.
- (73) Skone, J. H.; Govoni, M.; Galli, G. Self-consistent hybrid functional for condensed systems. *Phys. Rev. B* **2014**, *89*, 195112.
- (74) Skone, J. H.; Govoni, M.; Galli, G. Nonempirical range-separated hybrid functionals for solids and molecules. *Phys. Rev. B* **2016**, *93*, 235106.
- (75) Brawand, N. P.; Vörös, M.; Govoni, M.; Galli, G. Generalization of Dielectric-Dependent Hybrid Functionals to Finite Systems. *Phys. Rev. X* **2016**, *6*, 041002.
- (76) Shapley, W. A.; Chong, D. P. PW86–PW91 density functional calculation of vertical ionization potentials: Some implications for present-day functionals. *Int. J. Quant. Chem.* **2001**, *81*, 34–52.